

# Optimal design of pitched roof frames with tapered members using ECBO algorithm

Ali Kaveh\*, Vahid Reza Mahdavi and Mohammad Kamalinejad

Centre of Excellence for Fundamental Studies in Structural Engineering, Iran University of Science and Technology, Tehran, Iran

(Received August 16, 2016, Revised November 10, 2016, Accepted November 27, 2016)

**Abstract.** Pitched roof frames are widely used in construction of the industrial buildings, gyms, schools and colleges, fire stations, storages, hangars and many other low rise structures. The weight and shape of the gable frames with tapered members, as a familiar group of the pitched roof frames, are highly dependent on the properties of the member cross-sectional. In this work Enhanced Colliding Bodies Optimization (ECBO) is utilized for optimal design of three gable frames with tapered members. In order to optimize the frames, the design is performed using the AISC specifications for stress, displacement and stability constraints. The design constraints and weight of the gable frames are computed from the cross-section of members. These optimum weights are obtained using aforementioned optimization algorithms considering the cross-sections of the members and design constraints as optimization variables and constraints, respectively. A comparative study of the PSO and CBO with ECBO is also performed to illustrate the importance of the enhancement of the utilized optimization algorithm.

**Keywords:** gable frames; optimal design; meta-heuristic algorithms; tapered members; enhanced colliding bodies optimization algorithm

## 1. Introduction

Advances in science and technology, and the need to benefit from products based on new developments, entail the construction of safe and economic physical spaces for industrial buildings. By the end of World War II, countries became engaged in the reconstruction of the ruins of the war. Due to the extent of damage, the conventional methods were not sufficient for providing suitable residential and industrial spaces. This was the time when the industrialized countries started to think of producing buildings in harmony with other industrial manners for passing from the housing crisis. This led to construction of the low-rise metal buildings. Buildings are often considered as low-rise when their heights are less than 18 m. Sloped roof frames are the most common for low rise buildings, can be categorized based on their shapes: gable frames, mono slope frames, lean-to frames, saw tooth frames, domed frames, T-shape frames. These frames may have symmetrical or unsymmetrical geometry.

All of these frames, except T-shaped frames, may have one or two middle floors called mezzanines. The members of these frames are categorized as prismatic or non-prismatic sections. In non-prismatic type, the cross-section continuously vary from bottom to top (start to end) of members, and in prismatic type, the member has the same geometrical characteristics along the member (Fraser 1983, Watwood 1985).

In the field of structural optimization, there are many

methods to optimize the weight/cost of the structures, such as gradient-based and stochastic optimizers (Spires and Arora 1990, Saka and Geem 2013, Kazemizadeh Azad and Hasançebi 2015a). Since 1960s a vast amount of research has been carried out in the area of structural optimization, majority of which deal with minimizing the weight of the structures. The last two decades were highlighted by the development and improvement of the metaheuristic methods. Most of them deal with optimal design of two/three dimensional structures such as trusses, frames, dams, etc. (Kaveh 2016, Saka and Dogan 2012). A small fraction of the published papers are on gable frame structures with tapered members. Therefore, optimal design of the gable rigid frame with web-tapered members in the low rise buildings can be considered as an interesting and challenging issue in structural engineering research (Saka 1997, McKinstry *et al.* 2016).

The main objective of this paper is to find the optimum member sections of a symmetric gable frames by considering different alternatives based on the number of member divisions. The members of these frames are also considered as the web-tapered I-section members. The design method used in this study is also consistent with ASCE/SEI 7-10 (2010) and AISC-LRFD (1999) Specifications. Three metaheuristic algorithms consisting of the Particle Swarm Optimization (PSO), Colliding Bodies Optimization (CBO) and Enhance Colliding Bodies Optimization (ECBO) algorithms are utilized for finding the optimum weight of frames. CBO belongs to a family of meta-heuristic algorithms which were recently developed. Simple formulation and no internal parameter tuning are the main features of this algorithm (Kaveh and Mahdavi 2014, 2015). The ECBO is introduced by Kaveh and Ilchi

---

\*Corresponding author, Professor  
E-mail: [alikaveh@iust.ac.ir](mailto:alikaveh@iust.ac.ir)

Ghazaan (2014) and it uses memory to save some historically best solution to improve the performance of the CBO. Gholizadeh *et al.* (2016) optimized double layer barrel vaults considering nonlinear behavior. Gholizadeh and Milany (2016) presented optimal performance-based design of steel frames using different metaheuristics.

It should be noted that, since the plan rectilinear shape of gable frame depends on the dimensions of the sections, this work can be considered as the shape optimization of gable frames. In such a gable frame design problem, selecting appropriate cross-sections for the members is important because it influences the structural analysis and weight of the gable frame. Therefore, it is often necessary to find the best set of cross-sections for reducing the weight of gable frames and achieving an optimal and economical design.

The remainder of this paper is organized as follows: In section 2, the mathematical formulations of the structural optimization of the gable rigid frame problems are presented and a brief explanation of the ASCE/SEI 7-10 and AISC-LRFD 99 specifications is provided. Section 3 consists of the loading of the structures. Then an explanation of the enhance colliding bodies algorithm is presented in section 4. In section 5 the design examples and the discussions on the results are presented. Section 6 concludes the research.

## 2. Gable rigid frame optimization problems

The optimization problem can formally be stated as follows

$$\begin{aligned} &\text{Find} && X = [x_1, x_2, x_3, \dots, x_n] \\ & && \text{to minimize } Mer(X) = f(X) \times f_{penalty}(X) \\ &\text{subjected to} && g_i(X) \leq 0, i=1,2,\dots,m \end{aligned} \quad (1)$$

$$x_{imin} \leq x_i \leq x_{imax}$$

where  $X$  is the vector of design variables with  $n$  unknowns  $[x_1, x_2, x_3, \dots, x_n]$ ,  $g_i$  is the  $i$ th constraint from  $m$  inequality constraints and  $Mer(X)$  is the merit function;  $f(X)$  is the cost;  $f_{penalty}(X)$  is the penalty function which results from the violations of the constraints corresponding to the response of the gable rigid frames. Also,  $x_{imin}$  and  $x_{imax}$  are the lower and upper bounds of the design variables vector, respectively.

The exterior penalty function method is employed to transform the constrained optimization problem into an unconstrained one as follows

$$f_{penalty}(X) = 1 + \gamma_p \sum_{i=1}^m \max(0, g_j(x)) \quad (2)$$

where  $\gamma_p$  is penalty multiplier.

### 2.1 Objective function of the problem

In the gable frame design many factors affect the

construction cost of the project, the cost of the frames, foundation, purlins, girts, etc. However the main cost belongs to the structural frames. This cost in turn includes different items such as the frame steel, and the cutting, fabrication, installation, connections, etc. of the frame. Among all the aforementioned items, the most effective parameter is the steel due to the repetition of a frame in consecutive bays. Moreover, the weight of foundation and the seismic behavior of structure are significantly dependent upon the weight of the gable frames (Hwang *et al.* 1991). Therefore, the weight of gable frame structures is considered as the objective function in order to reduce the construction cost of the pitched roof frames. The weight of a gable frame structure can be expressed as

$$f(X) = \sum_{i=1}^n \rho V_i = \sum_{i=1}^n \rho \bar{A}_i l_i \quad (3)$$

where  $\rho$  is weight per volume of steel,  $V_i$  and  $l_i$  are the volume and length of the  $i$ th segment of the rigid frame structure, respectively,  $\bar{A}_i$  is the average of starting and ending cross section areas of the  $i$ th segment,  $n$  is the total number of segments in a gable frame.

### 2.2 Design constraints

Design constraints are divided into some groups including the deflection, strength and stability constraints. The strength and displacement constraints for steel frames are imposed according to the provisions of LRFD-AISC specifications (AISC 1999). These constraints are briefly explained in the following:

#### (a) Maximum vertical displacement of the pitched roof

$$\frac{\Delta_V}{L} - R_V \leq 0 \quad (4)$$

where  $\Delta_V$  is the maximum vertical displacement of roof;  $L$  is the length of span in the gable frame structure; and  $R_V$  is the allowable vertical displacement index which is equal to 1/360 and 1/240 under live and total loading, respectively.

#### (b) Maximum horizontal displacement

$$\frac{\Delta_H}{H} - R_H \leq 0 \quad (5)$$

where  $\Delta_H$  is the maximum horizontal displacement of eaves in the gable frame;  $H$  is the eaves height;  $R_H$  represents the allowable horizontal displacement index which considered as  $H/200$  under the all loadings.

#### (c) Strength constraints

$$\begin{cases} \frac{P_u}{2\phi_c P_n} + \frac{M_u}{\phi_b M_n} - 1 \leq 0, & \text{for } \frac{P_u}{\phi_c P_n} < 0.2 \\ \frac{P_u}{\phi_c P_n} + \frac{8M_u}{9\phi_b M_n} - 1 \leq 0, & \text{for } \frac{P_u}{\phi_c P_n} \geq 0.2 \end{cases} \quad (6)$$

where  $P_u$  is the required strength (tension or compression);  $P_n$  is the nominal axial strength (tension or compression);  $\phi_c$

is the resistance factor ( $\phi_c = 0.9$  for tension,  $\phi_c = 0.85$  for compression);  $M_u$  is the required flexural strength;  $M_n$  is the nominal flexural strength; and  $\phi_b$  denotes the flexural resistance reduction factor ( $\phi_b = 0.90$ ). The nominal tensile strength for yielding in the gross section is calculated by

$$P_n = A_g \cdot F_y \quad (7)$$

The nominal compressive strength of a member is computed as

$$P_n = A_g \cdot F_{cr} \quad (8a)$$

$$\begin{cases} F_{cr} = (0.658^{\lambda_c^2}) F_y, & \text{for } \lambda_c \leq 1.5 \\ F_{cr} = \left(\frac{0.877}{\lambda_c^2}\right) F_y, & \text{for } \lambda_c > 1.5 \end{cases} \quad (8b)$$

$$\lambda_c = \frac{kl}{r\pi} \sqrt{\frac{F_y}{E}} \quad (8c)$$

where  $A_g$  is the cross-sectional area of a member and  $k$  is the effective length factor.

#### (d) The buckling constraints

Considering the ANSI/AISC 341-10 (ASIC 2010) manual for design of slender compression elements, the reasonable and practical width-to-thickness ratios of  $\frac{b_f}{t_f} \leq 18$  and  $\frac{h}{t_w} \leq \frac{0.4E}{F_y} \leq 260$  are considered as the constraints this study. Here, the material characteristics are considered as:  $E=2.1e6$  kg/cm<sup>2</sup>;  $F_y=2520$  kg/cm<sup>2</sup>,  $\rho=7850$  kg/m<sup>3</sup>; and *Poisson's ratio*=0.3.

#### (e) The stability constraint

The stability constraints are considered in accordance with the ANSI/ AISC 360-10 (AISC 2010) manual. In designing the gable frames with web-taper, achieving the second-order analysis is one of the most significant aspects due to the offset of the cross-section central axis from the chord. This includes the matrix formulations based on the deformed geometry and the *P-delta* analysis procedures (Saffari *et al.* 2008). The *P-delta* effects cause the resulting additional force or moment in the members. Consider the following equation as an indicator of the magnitude of the expected stability index under *P-delta* effects

$$\theta = \frac{P_x \Delta I_e}{V_x h_{sx} C_d} \quad (9)$$

where  $\theta$  is the stability coefficient,  $P_x$  is the total vertical design load above level  $x$  with a maximum load factor of 1.0 (kip or kN),  $\Delta$  is the design story drift occurring simultaneously with  $V_x$ ,  $I_e$  is the importance factor,  $V_x$  is the seismic shear force acting between Levels  $x$  and  $x-1$ ,  $h_{sx}$  is the story height below level  $x$ , and  $C_d$  is the deflection amplification factor. The upper bound of the

stability coefficient ( $\theta_{\max}$ ) is determined as follows

$$\theta_{\max} = \frac{0.5}{\beta C_d} \leq 0.25 \quad (10)$$

where  $\beta$  is the ratio of shear demand to shear capacity for the story between levels  $x$  and  $x-1$ . This ratio is permitted to be conservatively taken as 1.0. If the stability coefficient,  $\theta$ , of a structure could be found equal or less than 0.1, the designer would ignore the second-order analysis. Where  $\theta$  is greater than 0.10 but less than or equal to  $\theta_{\max}$ , the incremental factor related to P-delta effects on displacements and member forces should be determined by the rational analysis. Alternatively, it is permitted to multiply displacements and member forces by  $1.0/(1-\theta)$ . Where  $\theta$  is greater than  $\theta_{\max}$ , the structure is potentially unstable and should be redesigned (AISC 2010). In this study, the deflection amplification factor,  $C_d$ , is considered as 4 due to the frame system. Also, the P-delta effect is considered on the seismic load combinations.

### 3. Structural loading

In this study, ASCE/SEI 7-10 (2010) manual is used for considering the dead, live, snow, wind and seismic loads and their influence on the gable frame. The applied loads on the gable rigid frame in low rise buildings generally consist of the vertical and horizontal loads, which are described in the follow subsections.

#### 3.1 The vertical loads

In accordance with the ASCE/SEI 7-10 (2010), the most effective vertical loads, which should be considered in the analysis process consist of:

- The dead loads including the self-weight of the structure and the weight of roof panel.
- The collateral loads including the false ceiling load and the weight of permanent appurtenance (i.e., R.T.U).
- The live loads
- The snow load
- The rain surcharge load

#### The dead and collateral loads (D)

For considering the dead and collateral loads, it is assumed that the type of cladding is a metal sandwich panel with a mass of 14.65 kg/m<sup>2</sup>. This load includes the purlins on the roof and there is no false ceiling. The collateral load was assumed zero. The dead load information is shown in Table 1.

#### The live loads (L)

According to the ASCE/SEI 7-10 (2010) manual, the live load of a pitched roof is 97.648 kg/m<sup>2</sup> (20 lb/ft<sup>2</sup>), and there is no concentrated load to check the rigid frames with it. It is also assumed that the live load is not reducible. The live load information is shown in Table 2.

**The snow load (SL)**

The snow loads consist of the balanced and unbalanced snow loads.

• *The balanced snow load*

The flat roof snow load,  $P_f$ , is evaluated by using the following equation

$$P_f = 0.7C_e C_t I_s P_g \tag{11}$$

where the exposure factor,  $C_e$ , thermal factor,  $C_t$ , and importance factor,  $I_s$ , are taken as 1.0 based on sections 7.3.1 through 7.3.3 of ASCE/SEI 7-10 manual. The ground snow load,  $P_g$ , determined per site-specific analysis is equal to  $97.65\text{kg/m}^2$  ( $20.0\text{lb/ft}^2$ ); thus:  $P_f = 14\text{psf}$ . The snow load acting on a sloping surface are assumed to act on the horizontal projection of that surface. The sloped roof (balanced) snow load,  $p_s$ , is calculated by multiplying the flat roof snow load,  $P_f$ , by the roof slope factor,  $C_s$  as

$$p_s = C_s P_f \tag{12}$$

The roof slope factor,  $C_s$ , is taken as 1.0 based on sections 7.4 of ASCE/SEI7-10; thus  $p_s = 14.0\text{psf}$  ( $68.353\text{kg/m}^2$ ).

• *The unbalanced snow loads*

As shown in Fig. 1, for hip and gable roofs with a slope exceeding 7 on 12 ( $30.2^\circ$ ) or with a slope less than 0.5 on 12 ( $2.38^\circ$ ) unbalanced snow loads are not required to be applied. Roofs with an eave to ridge distance,  $W$ , of less than 6.1 m (20ft) and having simply supported prismatic members, the spanning from ridge to eave should be designed to resist an unbalanced uniform snow load on the leeward side equal to  $1.P_g$ . For these roofs the windward side should be unloaded. For all other gable roofs, the unbalanced load should consist of  $0.3p_s$  on the windward side, and  $p_s$  on the leeward side plus a rectangular surcharge with magnitude  $\frac{h_d \gamma}{\sqrt{S}}$  and horizontal extent from the

ridge  $\frac{8}{3}h_d \sqrt{S}$ , where  $h_d$  is the drift height (Eq. (13)) which  $l_u$  is equal to the eave to ridge distance for the windward portion of the roof,  $W$ .

$$h_d = 0.433 \sqrt[3]{l_u^4 (p_g + 10)} - 1.5 \tag{13}$$

Thus:  $p_s = 68.353\text{kg/m}^2$ ,  $l_u = 8\text{m}$ ,  $P_g = 97.65\text{kg/m}^2$ ,  $S = 3.63$ ,  $h_d = 0.45\text{m}$ .

Table 1 Summary of the dead loading

Dead load ( $\text{kg/m}^2$ )	14.64
Loading per (m)	6
Uniform dead load ( $\text{kg/m}$ )	87.84

Table 2 Summary of the live loading

Live load ( $\text{kg/m}^2$ )	97.648
Load per (m)	6
Uniform live load ( $\text{kg/m}$ )	585.89

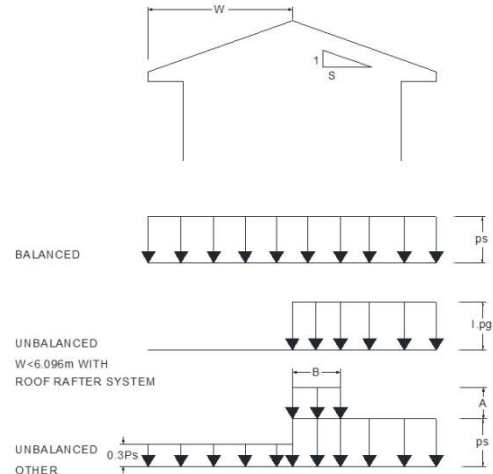


Fig. 1 Balanced and unbalanced snow loads for the gable roofs

**3.2 The lateral loads**

In accordance with ASCE/SEI 7-10, the most effective lateral loads, which should be considered in the analysis process, consist of:

• *The seismic load (E)*

The seismic base shear,  $V$ , in a given direction is determined according to the following equation

$$V = C_s W \tag{14}$$

where  $C_s$  and  $W$  are the seismic response coefficient and the effective seismic weight, respectively. The seismic response coefficient,  $C_s$ , is calculated as

$$C_s = \frac{S_{DS}}{R I_e} \tag{15}$$

where  $S_{DS}$  is the design spectral response acceleration parameter in the short period range,  $R$  is the response modification factor and  $I_e$  is the importance factor. Because of the location of this study is assumed to be Clay county Kansas in USA, the mapped Risk-Targeted Maximum Considered Earthquake (MCER) spectral response acceleration parameter for short periods ( $S_S$ ) and the mapped MCER spectral response acceleration parameter at a period of 1s ( $S_I$ ) are as 17% and 5%, respectively.

Table 3 The summarized calculation of  $C_s$

$S_{DS}$	0.2768
$R$	4.5
$I_e$	1
Maximum $C_s$	0.041
Minimum $C_s$	0.01
$\frac{S_{DS}}{R I_e}$	0.079
Then $C_s =$	0.041

Then, the  $S_{DS}$  values are evaluated as 0.2768 and the summarized calculation of the  $C_s$  parameter is shown in Table 3.

• *The wind loads (W)*

For evaluating the wind load for a low rise building, the wind pressure is calculated with the following equation

$$q_z = 0.613K_zK_{zt}K_dV^2 \quad (N/m^2); V \text{ in m/s} \quad (16)$$

where  $K_d$  is the wind directionality factor,  $K_z$  is the velocity pressure exposure coefficient,  $K_{zt}$  is the topographic factor, and  $V$  is the basic wind speed. These parameters values used in this study are  $K_d=0.85$ ,  $K_z=0.93$ ,  $K_{zt}=1.0$  and  $V=90$  mph. In this case study  $q_z=16.365$  psf. The velocity pressure at height  $h=26.57$  ft,  $q_h$ , is also taken as 16.876 psf.

The design wind pressures for the frame system of an enclosed and partially enclosed rigid buildings at all heights is determined by the following equation

$$p = qGC_p - q_i(GC_{pi}) \quad (17)$$

where:

$q = q_z$  for the windward walls evaluated at height  $z$  above the ground ( $q=79.90$  kg/m<sup>2</sup>).

$q = q_h$  for the leeward walls, side walls, and roofs, evaluated at height  $h$  ( $q=82.398$  kg/m<sup>2</sup>).

$q_i = q_h$  for the windward walls, side walls, leeward walls, and roofs of enclosed buildings and for negative internal pressure evaluation in partially enclosed buildings ( $q_i=82.398$  kg/m<sup>2</sup>).

$q_i = q_z$  for the positive internal pressure evaluation in partially enclosed buildings where height  $z$  is defined as the level of the highest opening in the building that could affect the positive internal pressure. For positive internal pressure evaluation,  $q_i$  may conservatively be evaluated at height  $h$  ( $q_i=q_h=82.398$  kg/m<sup>2</sup>).

$G$  = gust-effect factor (=0.85).

$p$  = external pressure coefficient.

$(GC_{pi})$  = internal pressure coefficient=  $\pm 0.18$ .

Table 4 The coefficient of  $C_p$  in two orthogonal directions of wind

The directions of wind		$C_p$
Transvers wind direction (Case 1)	Windward wall	0.8
	Windward roof	-0.7
	Leeward roof	-0.5
	Leeward wall	-0.5
Transvers wind direction (Case 2)	Windward wall	0.8
	Windward roof	-0.18
	Leeward roof	-0.5
	Leeward wall	-0.5

Table 5 The wind load (kg/m) on the gable frame of this study

Surface No.	$GC_{pi} = +0.18$		$GC_{pi} = -0.18$	
	IPP* - Case1	IPP* - Case2	INP* - Case1	INP* - Case2
1	237.02	237.02	415.00	415.00
2	-383.15	-164.63	-205.17	13.35
3	-299.11	-299.11	-121.13	-121.13
4	-288.60	-288.60	-110.62	-110.62

\* IPP= Internal positive pressure, INP= Internal negative pressure

Pressure is applied simultaneously on the windward and leeward walls and on the roof surfaces. The coefficient of  $C_p$  is defined at two orthogonal directions of wind as shown in Table 4 based on the ASCE 7-10 specifications. The values of wind loading on the gable frame are shown in Table 5.

3.3 Loading combinations

In this study, basic combinations for strength design are considered based on the ASCE 7-10 manual. The term of  $0.2S_{DS}D$  in combinations 5 and 7 is added because of the consideration of vertical seismic load.

1.  $1.4D$
2.  $1.2D+1.6L+0.5(S \text{ or } R)$
3.  $1.2D+1.6(S \text{ or } R) + (L \text{ or } 0.8W)$
4.  $1.2D + 1.0W + L + 0.5(S \text{ or } R)$
5.  $(1.2 + 0.2 S_{DS})D + E + L + 0.2S$
6.  $0.9D+1.0W$
7.  $(0.9 - 0.2 S_{DS})D + E$

4. Enhanced colliding bodies optimization algorithm

The optimization of gable rigid frame with tapered web members is a complex problem because of a large search space, multiple local optima and corresponding constraints. In this paper a simple and efficient meta-heuristic is applied, the so-called enhanced colliding bodies' optimization (ECBO), to solve this problem. For comparative study and showing the complexity of the problem, the standard colliding bodies optimization (CBO) is also utilized. In the following, the ECBO algorithm is briefly introduced.

The colliding bodies optimization is based on the momentum and energy conservation law for 1-dimensional collision. This algorithm contains a number of Colliding Bodies (CB) with each one being treated as an object with specified mass and velocity which collided with others. After collision, each CB moves to a new position with new velocity with respect to old velocities, masses and coefficient of restitution (Kaveh and Mahdavi 2015).

In order to improve the CBO to obtain faster and more reliable solutions, Enhanced Colliding Bodies Optimization (ECBO) was developed which uses memory to save a number of historically best CBs and also utilizes a mechanism to escape from local optima. The steps of this technique are as follows:

**Level 1: Initialization**

**Step 1:** The initial positions of all the populations are determined randomly in the search space.

**Level 2: Search**

**Step 1:** The value of mass for  $k$ th CB,  $m_k$ , is evaluated as

$$m_k = \frac{1}{\sum_{i=1}^n \frac{1}{fit(i)}}, \quad k = 1, 2, \dots, 2n \quad (18)$$

where  $fit(i)$  represents the objective function value of the  $i$ th CB, and  $2n$  is the population size.

**Step 2:** Colliding memory (CM) is utilized to save a number of historically best population vectors and their related mass and objective function values. Solution vectors which are saved in CM are added to the population and the same number of current worst populations are removed. Finally, the populations are sorted according to their masses in a decreasing order.

**Step 3:** The CBs are divided into two equal groups: (i) stationary group, (ii) moving group. The first group is stationary and consists of good agents. This set of populations is stationary and their velocity before collision is zero. The second group consists of moving agents which move toward the first group.

**Step 4:** The velocities of stationary and moving bodies before collision are evaluated as

$$v_i = \begin{cases} 0, & i = 1, \dots, n \\ x_i - x_{i-n}, & i = n + 1, \dots, 2n \end{cases} \quad (19)$$

where,  $v_i$  and  $x_i$  are the velocity vector and position vector of the  $i$ th CB, respectively.

**Step 5:** The velocities of stationary and moving bodies after the collision are evaluated using the following equation

$$v'_i = \begin{cases} \frac{(m_{i+n} + \varepsilon m_{i+n})v_{i+n}}{m_i + m_{i+n}}, & i = 1, \dots, n \\ \frac{(m_i - \varepsilon m_{i-n})v_i}{m_i + m_{i-n}}, & i = n + 1, \dots, 2n \end{cases} \quad (20)$$

where,  $v_i$  and  $v'_i$  are the velocities of the  $i$ th CB before and after the collision, respectively.  $\varepsilon$  is the coefficient of restitution (COR) and is defined as the ratio of the separation velocity of the two agents after collision to approach velocity of two agents before collision. In this algorithm, this index is defined to control of the exploration and exploitation rates. For this purpose, the COR is decreased linearly from unit value to zero. Here,  $\varepsilon$  is defined as

$$\varepsilon = 1 - \frac{iter}{iter_{max}} \quad (21)$$

where  $iter$  is the actual iteration number, and  $iter_{max}$  is the maximum number of iterations. Here, COR is equal to unity and zero representing the global and local search, respectively. In this way, a good balance between the global

and local search is achieved by increasing the iteration.

**Step 6:** The new position of each CB is calculated by

$$x_i^{new} = \begin{cases} x_i + rand \circ v'_i, & i = 1, \dots, n \\ x_{i-n} + rand \circ v'_i, & i = n + 1, \dots, 2n \end{cases} \quad (22)$$

where,  $x_i^{new}$  and  $v'_i$  are the new position and the velocity after the collision of the  $i$ th CB, respectively.

**Step 7:** A parameter **Pro** within (0, 1) is introduced and it is specified whether a component of each CB must be changed or not. For each colliding body, **Pro** is compared with  $r_{ni}$  ( $i=1,2,\dots,n$ ) which is a random number uniformly distributed within (0, 1). If  $r_n < \mathbf{Pro}$ , one dimension of the  $i$ th CB is selected randomly and its value is regenerated as follows

$$x_{ij} = x_{j,min} + random.(x_{j,max} - x_{j,min}) \quad (23)$$

where  $x_{ij}$  is the  $j$ th variable of the  $i$ th CB, and  $x_{i,min}$  and  $x_{i,max}$  are the lower and upper bounds of the  $j$ th variable, respectively. In order to protect the structures of CBs, only one dimension is changed.

**Level 3: Terminal condition check.**

**Step 1:** After a predefined maximum evaluation number, the optimization process is terminated.

**5. Design examples**

In this study, one design example is considered for optimization by the PSO, CBO and ECBO algorithms. There are three alternatives for design that considers the different variables. The differences are member division, assignment and alignment. As appointed in Fig. 2 to Fig. 4, the numbers of variables are different in these alternatives and help to achieve the optimal design for the frames. The columns and rafters are web-tapered I-section that may have different inside and outside flange thickness with the same flange width.

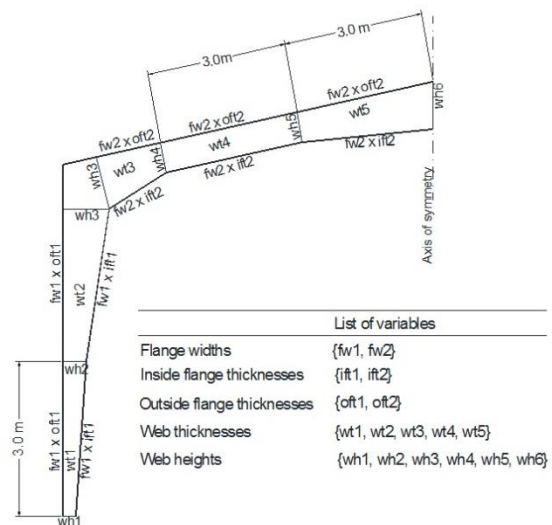


Fig. 2 The first alternative considered as variables

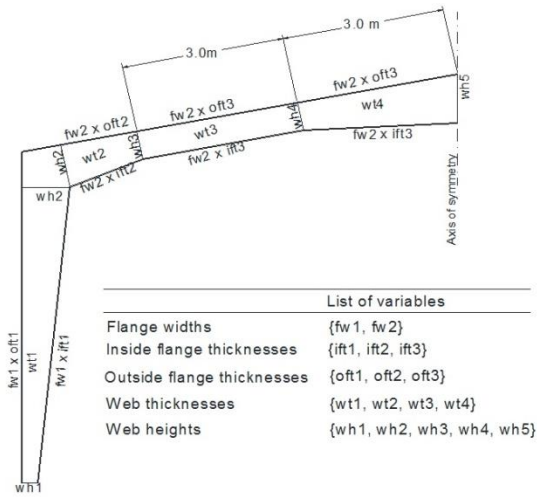


Fig. 3 The second alternative considered as variables

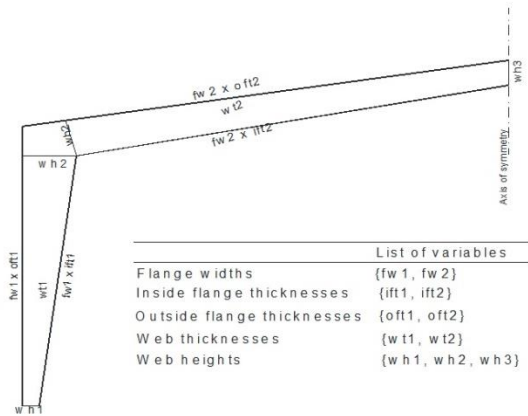


Fig. 4 The third alternative considered as variables

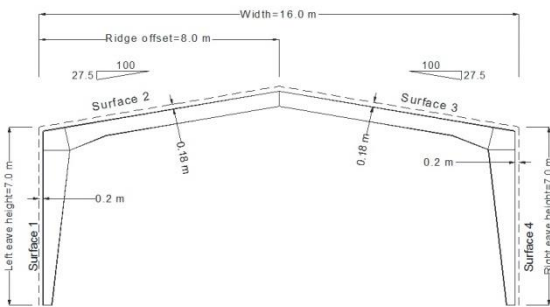


Fig. 5 The geometrical shape of the example building

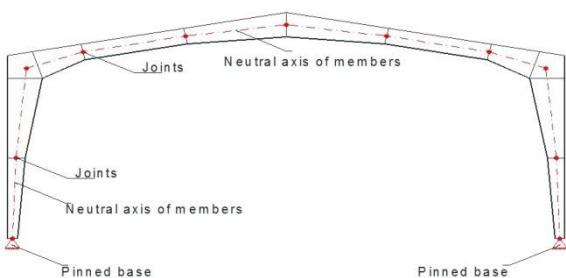


Fig. 6 An idealized model of a gable frame based on the neutral axis of members

All three frames had the same plan layout and geometrical data as shown in Fig. 5 and Table 6, with the bay width of 16 m, the eave height of 7 m and a ridge height of 9.2 m. The center-to-center spacing of the gable frames had 6m. The site location had county clay from Kansas in United States of America. As mentioned before, 17, 17 and 11 design variables are considered for the first, second and third alternatives, respectively. The number of Colliding Bodies (CB) or agents for these examples is considered 30. The maximum number of iterations is 100. Hence, the number of fitness function evaluation is  $30 \times 100 = 3000$ . For the sake of simplicity, the penalty approach is used for constraint handling. The optimization algorithms and the analysis and design of structures are coded in Matlab and SAP200 software, respectively. In the analysis process, a pin-based structural frame is constructed, and the nodal geometry of the members are given based on the neutral axis of the members. An idealized model of a gable frame is shown in Fig. 6.

For designing the gable frame, two major classes of design variables must be dealt with. The first class is geometric layout variables such as the length of spans or the slope of rafters, the second class is cross section design variables such as dimensions of the starting and ending sections of a segment. In the sizing optimization literature, design variables can be either continuous or discrete. In real applications, the designer is restricted to selecting the design variables (cross section sizes), from a pre-assigned list of available values (Kazemizadeh Azad and Hasançebi 2015b).

In this study, only the second class of design variables is considered as discrete sizing optimization. These design variables are the dimensions, i.e., the thickness and width of web and flange, of cross sections at the intersections of segments of gable frame. In order to make the optimal gable frame model practical, the thickness of webs and flanges should be selected from the discrete set  $T = \{0.5, 0.6, 0.8, 1, 1.2, 1.5, 2, 2.5, 3\}$  (cm), the width of webs should be selected from the discrete set  $WW = \{15, 20, 25, \dots, 115, 120\}$  (cm), and the width of flanges should be selected from the discrete set  $FW = \{15, 20, 25, \dots, 40, 45\}$  (cm). The web thicknesses should be selected equal or less than the flange thicknesses in all member sections for practical application.

Tables 7, 8 and 9 compare the results obtained using the PSO, CBO and ECBO algorithms for all of the examples. As discussed before and shown in these tables, the constraints of outcome of all algorithms are satisfied, and now the results can be compared. The outcomes of the ECBO algorithm are also better than those of the PSO and CBO with the same number of objective function evaluations. In addition comparing the results, it can be seen that the optimum weight of the ECBO in the first through third alternatives are respectively 10.81%, 9.76% and 24.64% lighter than those of the CBO. Also, the optimum weight obtained using the ECBO in the second and third alternatives are respectively 1.41% and 8.31% lighter than those of the first alternative, and these values are 0.45% and 21.83% for the CBO algorithm.

Table 6 The geometrical information of building shape

Eave height	7.0 m
Slope	27.5%
Width	16.0 m
Length	18.0 m
Bay spanning	3@6.0 m
Load width of the main frame	6.0 m
Ridge offset	8.0 m
Ridge height	9.2 m
Mean roof height	8.1 m
$\alpha$ =Wall offset in surface 1	0.2 m
$\beta$ = Roof offset in surfaces 2 and 3	0.18 m
$\gamma$ = Wall offset in surface 4	0.2 m
Roof slope angle at surface 2	15.37 degree
Roof slope angle at surface 3	15.37 degree

Table 7 Optimal design of three alternative examples using the ECBO algorithm

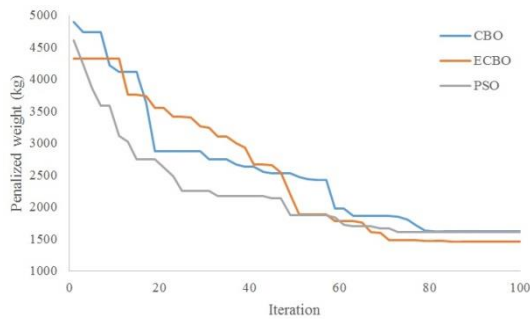
Case No.	Surface No.	Element type	Element No.	Start web height (m)	Flange width (m)	Inside flange thickness (m)	Web thickness (m)	Outside flange thickness (m)	End web height (m)	Weight (kg)
1	1	Column	1	0.15	0.2	0.008	0.005	0.006	0.8	1457.2
			2	0.8	0.2	0.008	0.005	0.006	1.2	
			3	1.2	0.15	0.01	0.006	0.01	0.85	
	2	Beam	4	0.85	0.15	0.01	0.005	0.01	0.35	
			5	0.35	0.15	0.01	0.005	0.01	1.05	
2	1	Column	1	0.35	0.25	0.008	0.005	0.008	1.1	1477.8
			2	1.1	0.15	0.008	0.005	0.008	1.2	
	2	Beam	3	1.2	0.15	0.008	0.005	0.008	0.45	
			4	0.45	0.15	0.008	0.005	0.008	0.3	
3	1	Column	1	0.65	0.2	0.008	0.005	0.008	0.95	1578.4
	2	Beam	2	0.95	0.25	0.008	0.005	0.008	0.3	

Table 8 Optimal design of three alternative examples using the CBO algorithm

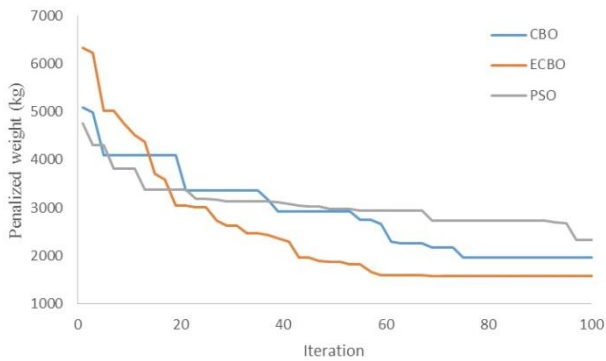
Case No.	Surface No.	Element type	Element No.	Start web height (m)	Flange width (m)	Inside flange thickness (m)	Web thickness (m)	Outside flange thickness (m)	End web height (m)	Weight (kg)
1	1	Column	1	0.15	0.15	0.006	0.006	0.01	1.2	1614.8
			2	1.2	0.15	0.01	0.005	0.01	1.1	
			3	1.1	0.15	0.01	0.006	0.01	1.2	
	2	Beam	4	1.2	0.15	0.01	0.005	0.01	0.3	
			5	0.3	0.15	0.01	0.006	0.01	0.95	
2	1	Column	1	0.35	0.2	0.015	0.005	0.03	1.2	1622.14
			2	1.2	0.45	0.025	0.005	0.03	0.75	
	2	Beam	3	0.75	0.45	0.01	0.01	0.005	0.45	
			4	0.45	0.45	0.01	0.005	0.005	1.2	
3	1	Column	1	0.15	0.2	0.015	0.008	0.01	0.9	1967.3
	2	Beam	2	0.9	0.25	0.01	0.006	0.01	0.35	

Table 9 Optimal design of three alternative examples using the PSO algorithm

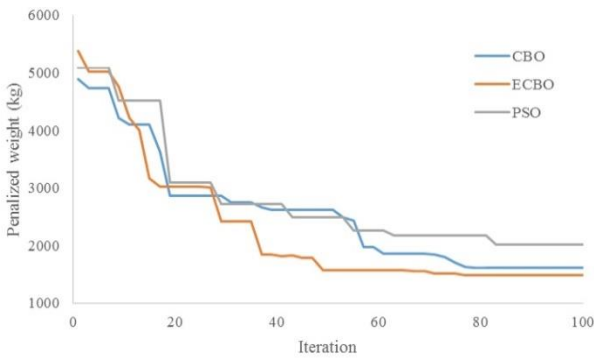
Case No.	Surface No.	Element type	Element No.	Start web height (m)	Flange width (m)	Inside flange thickness (m)	Web thickness (m)	Outside flange thickness (m)	End web height (m)	Weight (kg)
1	1	Column	1	1	0.15	0.01	0.005	0.012	0.75	1605.21
			2	0.75	0.15	0.01	0.005	0.012	1.15	
			3	1.15	0.15	0.006	0.006	0.01	0.75	
	2	Beam	4	0.75	0.15	0.006	0.008	0.01	0.8	
			5	0.8	0.15	0.006	0.005	0.01	0.2	
2	1	Column	1	0.8	0.2	0.015	0.006	0.02	0.85	2140.73
			2	0.85	0.90	0.025	0.008	0.02	0.40	
	2	Beam	3	0.40	0.90	0.015	0.012	0.015	0.45	
			4	0.45	0.90	0.015	0.012	0.006	0.4	
3	1	Column	1	0.50	0.2	0.025	0.005	0.015	0.85	2019.17
	2	Beam	2	0.85	0.45	0.02	0.005	0.02	0.80	



(a)



(b)



(c)

Fig. 7 The convergence rate of the PSO, CBO and ECBO for: (a) first, (b) second and (c) third alternative

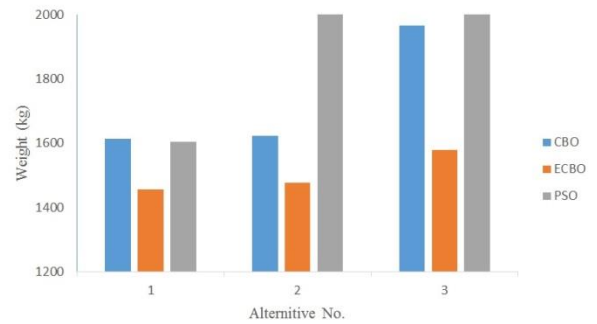


Fig. 8 Comparison of optimal weights obtained using PSO, CBO and ECBO for three alternatives

Fig. 7 shows the convergence rates of the best penalized weights obtained using all algorithms in the optimization process for all the alternatives. It can be seen from this figure that though the PSO and CBO algorithms are considerably faster in the early optimization iterations, the ECBO algorithm converged to a significantly better design in the later optimization iterations without being trapped in local optima. Fig. 8 compares the optimal weights obtained using all algorithms for all alternatives. As mentioned before, the design variables and the number of member divisions are decreased in the first through third alternatives. It can also be observed that the optimal weight is decreased by increasing the number of member divisions.

### 6. Conclusions

An efficient optimization method is proposed for optimal design of the symmetric gable frames for tapered-web I-section members, based on Colliding Bodies Optimization (CBO) and Enhanced Colliding Bodies Optimization (ECBO) algorithms. The CBO mimics the laws of collision between bodies. The very simple implementation and parameter independency are definite strength points of CBO. In the ECBO, some strategies have been achieved to promote the exploitation ability of the CBO.

In order to find the optimal cross section sizes of the

gable frames, the weight of gable frame and cross section sizes are respectively defined as the objective function and variables in the optimization process. Then, the cross section sizes are selected based on optimization algorithms from practical available discrete variables.

The validity and efficiency of the proposed method are shown through three alternative examples with different member divisions of the members for the test problem. The outcomes are that all the algorithms could decrease the weight of the real gable frames without appearing to violate any constraint. Moreover, the ECBO algorithm clearly outperforms the PSO and CBO algorithms with the same computational time, which shows the importance of selecting the effective optimization algorithm for this problem. Also, the optimal weight is decreased by increasing the number of member division and the decision variables in the gable frame. Future researches can investigate problems such as, optimization other types of the gable frames using recently developed metaheuristic optimization algorithms.

## Acknowledgments

The first author is grateful to the Iran National Science Foundation for the support.

## References

- AISC. (1999), "Load and Resistance Factor Design Specification for Structural Steel Buildings", *American Institute of Steel Construction*, Chicago, IL.
- AISC. (2010), "Specification for Structural Steel Buildings, ANSI/AISC 360-10", *American Institute of Steel Construction*, Chicago, IL.
- ASCE 7-10. (2010), "Minimum design loads for building and other structures", *American Society of Civil Engineers.*, Reston, Virginia.
- Gholizadeh, S., Gheytratmand, C. and Davoudi, H. (2016), "Optimum design of double layer barrel vaults considering nonlinear behavior", *Struct. Eng. Mech.*, **58**, 1109-1126.
- Gholizadeh, S. and Milany, A. (2016), "Optimal performance-based design of steel frames using advanced metaheuristics", *Asian J. Civil. Eng.*, **17**, 607-624.
- Hasançebi, O., Çarbaş, S., Doğan, E., Erdal, F. and Saka, M.P. (2010), "Comparison of non-deterministic search techniques in the optimum design of real size steel frames", *Comput. Struct.*, **88**(17-18), 1033-1048.
- Hwang, J., Chang, K. and Lee, G. (1991), "Seismic behavior of gable frame consisting of tapered members", *J. Struct. Eng.*, **117**(3), 808-821.
- Kaveh, A. (2017), "Advances in metaheuristic algorithms for optimal design of structures", 2<sup>nd</sup> Ed., Springer, Switzerland.
- Kaveh, A. and Ilchi Ghazaan, M. (2014), "Enhanced colliding bodies optimization for design of continuous and discrete variables", *Adv. Eng. Softw.*, **77**, 66-75.
- Kaveh, A. and Mahdavi, V.R. (2014), "Colliding bodies optimization: A novel meta-heuristic method", *Comput. Struct.*, **139**, 18-27.
- Kaveh, A. and Mahdavi, V.R. (2015), "Colliding Bodies Optimization; Extensions and Applications", Springer, Switzerland.
- Kazemizadeh Azad, S. and Hasançebi, O. (2015a), "Discrete sizing optimization of steel trusses under multiple displacement constraints and load cases using guided stochastic search technique". *Adv. Eng. Softw.*, **52**(2), 383-404.
- Kazemizadeh, S. and Hasançebi, O. (2015b), "Computationally efficient discrete sizing of steel frames via guided stochastic search heuristic", *Comput. Struct.*, **156**, 12-28.
- Fraser, D. (1983), "Design of tapered member portal frames", *J. Construct. Steel Res.*, **3**(1), 20-26.
- McKinstry, R., Lima, J.B.P., Tanyimboh, T., Phanc, D.T. and Sha, W. (2016), "Comparison of optimal designs of steel portal frames including topological asymmetry considering rolled, fabricated and tapered sections", *Eng Struct.*, **111**, 505-524.
- Saffari, H., Rahgozar, R. and Jahanshahi, R. (2008), "An efficient method for computation of effective length factor of columns in a steel gabled frame with tapered members", *J. Constr. Steel Res.*, **64**(4), 400-406.
- Saka, M. (1997), "Optimum design of steel frames with tapered members", *Comput. Struct.*, **63** (4), 798-811.
- Saka, M.P. and Dogan, E. (2012), "Recent developments in metaheuristic algorithms: a review", *Comput. Tech. Rev.*, **5**, 31-78.
- Saka, M.P. and Geem, Z.W. (2013), "Mathematical and metaheuristic applications in design optimization of steel frame structures: an extensive review", *Math. Probl. Eng.*, **2013**, 33 pages Article ID 271031.
- Spires, D. and Arora, J. (1990), "Optimal design of tall rc-framed tube buildings", *J. Struct. Eng. - ASCE*, **4**, 877-897.
- Watwood, V. (1985), "Gable frame design considerations", *J. Struct. Eng. - ASCE*, **7**, 1543-1558.

CC